Hyphenating paper-based biosensors with smartphones

Michael J. Dillon[a,*] **and Katrina Campbell**[b]
[a]Peninsula Medical School, University of Plymouth, Plymouth, United Kingdom
[b]Institute for Global Food Security, Queen's University Belfast, Belfast, United Kingdom
*Corresponding author: e-mail address: michael.dillon@plymouth.ac.uk

Contents

1. Introduction

Paper-based biosensors are microfluidic devices designed from cellulose and nitrocellulose fibres [1]. They are commonly used for on-site, non-laboratory-based testing because they are light-weight, robust, inexpensive, small-in-size (millimetres or centimetres) and highly portable. Additionally, they can be created from biodegradable renewable resources [2], and they can accommodate a range of liquid sample types, including biological (e.g., blood, urine, saliva, sputum), environmental (e.g., water, soil)

Comprehensive Analytical Chemistry
ISSN 0166-526X
https://doi.org/10.1016/bs.coac.2022.11.002

and chemical (e.g., clinical and veterinary medicines). Using paper also has the benefit of filtering out environmental contaminants from samples. These qualities also align with the World Health Organization's ASSURED criteria (Affordable, Sensitive, Specific, User-friendly, Rapid & Robust, Equipment free, Deliverable) [3], making them excellent diagnostic tests for resource-poor settings. Indeed, paper-based biosensors have a range of uses, including clinical diagnostics, veterinary diagnostics, environmental sampling, and food safety. Recently, smartphones have been identified as an important way to be complimentary for the enhancement of data that can be collated from these devices to make paper-based biosensors even more useful.

2. Paper-based biosensors

There are many different types of paper-based diagnostics, but they all function on a similar principle: fluid is placed on an inlet, and then transferred across a membrane, usually through capillary action, to an outlet where a chemical or biochemical reaction takes place. Some tests can even be multiplexed to provide more than one reaction or result. The reactions are usually colorimetric and can be seen with the naked eye. Paper is particularly beneficial for colorimetric analysis: it is normally white, which provides strong contrast for colour-change based detection. Broadly, paper-based diagnostics can be separated into the three categories depending on how they are designed: the dipstick assay, the lateral flow device (LFD), and microfluidic paper-based analytical devices (μPADs) (Fig. 1).

2.1 The dipstick assay

The dipstick assay is widely cited as a simple, low-cost diagnostic tool. It is comprised of a water-resistant plastic backing, lined with multiple absorbent pads embedded with chemical reagents (Fig. 1A). The assay is briefly placed into a liquid sample and then removed; analytes from the sample interact with the embedded chemical reagents to provide a colorimetric change that indicates a result. Dipsticks can contain more than one assay on each stick. One of the most common examples is litmus paper. Litmus paper is impregnated with chemicals that change colour depending on the pH of the solution; this is because the pH alters how protonated the chemical is [4]. For example, at a low pH, bromothymol blue is fully protonated and has a yellow colour; however, at higher pH's, bromothymol blue loses protons and shifts to a blue colour.

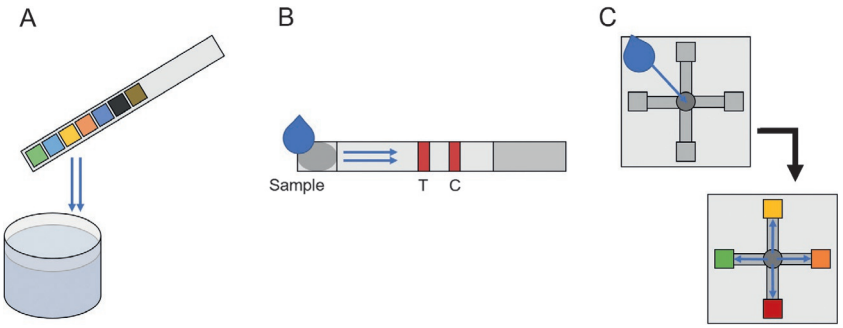

Fig. 1 Examples of different types of paper-based biosensor. (A) The dipstick assay is briefly submerged into a liquid sample. It has multiple discrete zones for sample analysis, typically via chemical reagents embedded on small nitrocellulose membranes attached to a plastic backing card. Analytes in the sample interact with the embedded chemical reagents to change the colour gradient and indicate a positive or negative result. (B) A small liquid sample is placed into the sample port of the lateral flow assay. Capillary action pulls the liquid sample across a series of membranes where there is a test line (T) and a control line (C) to indicate results, usually by immunological reactions. (C) μPADs range from relatively simple to very complex paper-based devices. In most cases, a liquid sample is placed into a sample port. Capillary action draws the sample through a series of channels, where various chemical reactions can provide discrete results, or build upon each other in a multi-step reaction to produce a result.

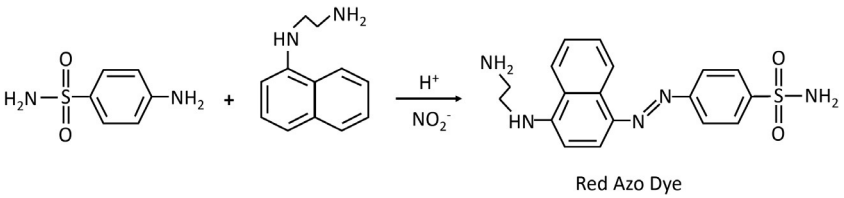

Fig. 2 The Griess Reagent system uses sulfanilamide and N-1-naphthylethylenediamine dihydrochloride, in conjunction with nitrites and acidic conditions, to produce a red coloured azo dye. The reaction cannot proceed without a nitrite intermediary; therefore, the sample pad will only turn red in the presence of nitrites.

The urinalysis dipstick assay is another commonly used dipstick assay. It is a screening tool for urinary tract infection (UTIs) [5]. UTIs are caused by gram-negative bacteria that convert urine nitrates into nitrites. Here, the absorbent pad contains Griess reagent. A urine sample is placed on the paper: nitrites interact with the Griess reagent [6] to produce a red coloured azo dye (Fig. 2). Urine does not normally contain nitrites, therefore, if nitrites are detected, it is likely due to a bacterial infection [7].

The urine dipstick assay commonly includes additional tests for blood, ketones, glucose, pH, protein, bilirubin, urobilinogen, and/or leukocyte esterase, all on the same test strip. The dipstick assay has also been adapted for many purposes, for example, to detect pathologies in animals [8] and to monitor environmental pesticides [9,10].

2.2 The lateral flow device (LFD)

The lateral flow device (LFD) is more complex than the dipstick assay. It is comprised of multiple different membranes arranged linearly (Fig. 1B). A liquid sample is placed at one end of the device, and capillary action moves the sample across various zones on the device, where different reactions can take place. Briefly, the different zones of the test are:

1. The sample pad. A liquid sample is placed on this pad, which controls the distribution of the sample flow to the rest of the test. In addition, reagents can be embedded here and once the sample pad is wet, can then be released to flow across the device.
2. The conjugation pad. Here, analytes in the sample interact with a detection molecule that can indicate their presence (or lack thereof).
3. A test line. Here, the final reactions take place to indicate a positive or a negative result. Some tests can have more than one test line.
4. A control line. This zone indicates that the liquid sample has successfully moved across the test in sequential order to completion.
5. An absorbent pad. This pad controls the sample flow rate across the membranes via capillary action and catches any excess fluid.

2.2.1 Detection molecules

Detection molecules can be a variety of different molecules, including antibodies, aptamers, and even nucleotide sequences. When antibodies are used, the test is often called a lateral flow immunoassay (LFIA). Antibodies are small immune proteins that bind to an analyte. They are a natural, adaptive immune response in vertebrates [11]. They have been used in bioanalysis for over five decades because they are easy to produce and can be highly specific [12] to chosen targets. There are two types of antibodies used in the LFIA: polyclonal antibodies (pAbs) and monoclonal antibodies (mAbs). PAbs are generated in vivo by immunising an animal, most commonly a rabbit or sheep, with the analyte of interest, and then by purifying the resultant antibodies from the animal's blood. This has the advantage of being very quick, however, due to the polyclonal nature, batch-to-batch consistency can vary [13,14]. MAbs are similarly generated by immunising an animal, usually

mice, with an analyte of interest, however, here, the antibody producing cells, the B lymphocytes, are harvested and immortalised, meaning the antibodies can be produced in vitro forever [12]. This method ensures more robust batch-to-batch consistency, however, there can still be some genetic drift. Thus each batch of pAbs or mAbs needs to be thoroughly validated after production and purification [13,14].

Aptamers are short single-stranded DNA or RNA that can be designed with specific 3-dimensional conformations that bind to an analyte [15,16]. Aptamers are 10 to 100 nucleotides in length, depending on the analyte size, and, like antibodies, they can be very specific to their target. Indeed, aptamers can be used as a substitute for antibodies for all bioanalysis applications, and in some cases are superior. Aptamers are smaller in size, meaning that more individual molecules can be used to detect the antigen, potentially making the test more sensitive. Additionally, because aptamers are nucleotide sequences, they are more stable, particularly at high temperatures, making for a more robust diagnostic test with a longer shelf-life. Furthermore, aptamers lack immunogenicity, and thus are less likely to cross react with other biological molecules in the sample. Finally, once an aptamer has been identified, it is much easier to ensure consistent reproduction and batch-to-batch consistency. That said, identifying suitable aptamers can be much more difficult. This point should not be taken lightly. Aptamers are produced in vitro, utilising a combinatorial DNA library and a technique called Systematic Evolution of Ligands Exponential Enrichment (SELEX) [17,18]. SELEX can be inefficient, making it difficult to develop high affinity aptamers to specific targets [19–21]. However, this has been an area of constant improvement over the past two decades with multiple modified methods showing increasing promise [22].

Antibodies or aptamers can be used in conjunction with nucleotide acid sequences to produce a nucleic acid lateral flow immunoassay (NALFIA). In this type of assay, haptens are incorporated into DNA primers targeting specific nucleotide sequences. If the sequence is present during PCR-amplification, the resultant product will have haptens on either side of the DNA sequence; antibodies or aptamers can then capture and label the complex by binding with the hapten. For example, Seidel et al. [23] developed a NALFIA to rapidly detect methicillin resistance genes in bacterial samples. Their method was more sensitive and significantly faster than traditional assays, such as culture or real-time PCR. The hapten does not always have to interact with an antibody; other reactions can be suitable. For example, the hapten can be biotin with avidin as the capture or detector molecule [24].

2.2.2 Visual labels

Regardless of which detection molecule is used, it must be conjugated to a visual marker. There are a myriad of visual labels available to use. The most common labels provide a colorimetric change with the naked eye; for example, colloidal gold nanoparticles are the most common visual markers for reporting LFIA results. They come in a variety of sizes (nanometre scale) and are spherical in shape. They are environmentally friendly, easy to produce, and can be functionalised for conjugation to an antibody or aptamer. Colloidal gold nanoparticles have a signature red colour that can easily be seen with the naked eye. Other examples of visual markers that can be seen with the naked eye include coloured latex beads [25], carbon nanoparticles [26–28], carbon nanotubes [29], and enzymes [30]; the different sizes and structures have different nanostructures to improve binding capacity depending on the antigen. Uniquely, enzymes have been used for chemiluminescence detection, for example Kawde et al. [30] used horseradish peroxidase labelled antibodies to detect carcinoembryonic antigen in human plasma. Here, the benefits of using an enzyme assay improved sensitivity compared to colloidal gold, however, at the same time it increases the complexity of the assay with multiple time-limited steps and a development phase.

When used with the naked eye, these tests are qualitative, providing a simple yes or no answer to whether the analyte of interest is present. Some tests can become semi-quantitative by including a gradient card with pre-printed lines of varying intensity that correspond with a numerical result. This is very similar to a dipstick assay, whereby the user can visually compare the intensity of their test line to a known standard. However, it can be difficult to get accurate results; most dipstick assays rely on a range of colour changes to delineate ranges more clearly, whereby the user is comparing line colour intensity. As an alternative, some tests can include an optical reader, such as a handheld camera device [31] or even a smartphone camera [32], which can take away some of the subjectivity in analysing the results and also produce more accurate quantitation if needed.

Similarly, magnetic nanoparticles as a label can be used both by the naked eye and with external devices to understand the test results [33]. Magnetic particles can be coloured, to produce a test line result that is visible to the naked eye or by an optical reader. Uniquely, the magnetic signals at the test line can also be used as a signal and detected by a magnetic reader. Reportedly, these signals are more stable compared to optical signals and significantly more sensitive [34]. This means the test can be stored for long periods of time and the results reviewed again at a future date.

There are also many different types of visual marker that can't be seen with the naked eye but are still useful. For example, fluorescent molecules can sometimes be more sensitive than colloidal gold due to the very strong signal each individual molecule emits. That said, with these devices, the labels absolutely require an external device that can excite fluorophores and detect the emission. They also suffer from decreased stability and photobleaching [35]. More recently, quantum dots have been developed to address some of these shortcomings. For example, due to their inorganic nature, they are more stable and more resistant to photobleaching [36]. However, they can be more difficult to conjugate to detection molecules [37], and thus are not so widely used yet. Other examples of this type of label include lanthanide chelate labels [38], up-converting phosphor [39], and fluorochrome dye [40].

2.2.3 LFIA formats

There are two main types of lateral flow assay, the sandwich assay and the competitive assay (Figs. 3 and 4). Sandwich assays are normally used for larger analytes because they have multiple binding sites and thus can accommodate multiple molecules binding simultaneously. Common examples include hormone testing [41], infectious disease antigens [42], and food

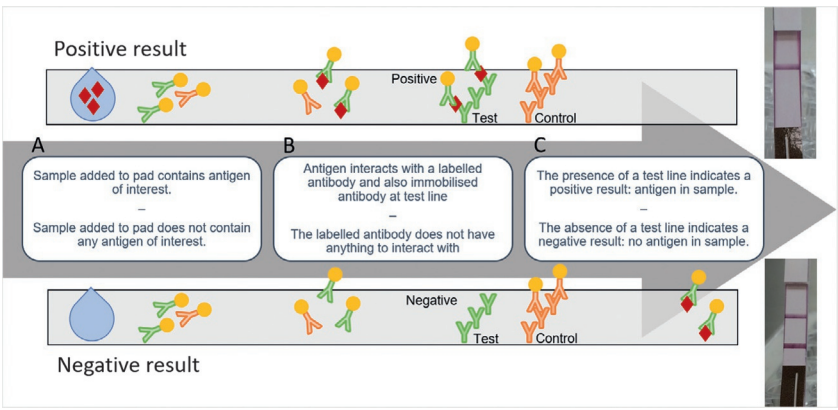

Fig. 3 Examples of positive and negative lateral flow sandwich immunoassay results. Results are dependent on the presence of an antigen: if there is antigen in the sample, it is 'sandwiched' between two antibodies at the test line, producing a colour change to indicate the positive result. Conversely, if there is no antigen in the sample, a 'sandwich' cannot be built at the test line, and thus there is no colour change, and a negative result is achieved. This format is particularly useful for larger antigens that can accommodate multiple binding sites.

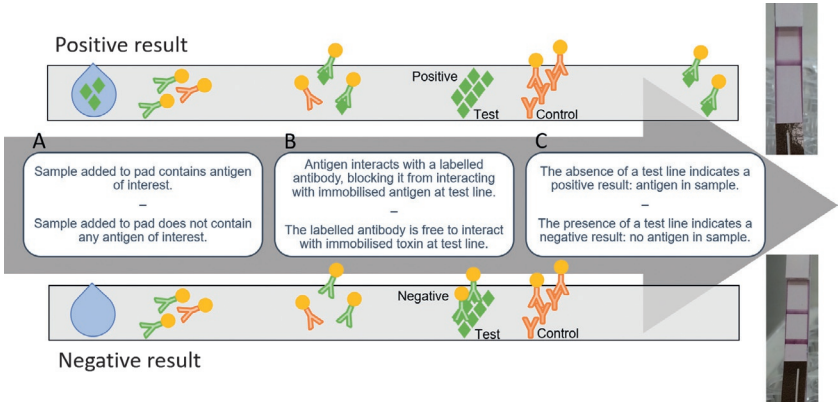

Fig. 4 Examples of positive and negative competitive lateral flow immunoassay results. Results are inverse compared to a sandwich assay. Results are still dependent on the presence of an antigen: in this format, if there is antigen in the sample, it will bind with the labelled antibody, preventing the antibody from interacting at the test line. Thus, there will be no colour change at the test line. Conversely, if there is no antigen in the sample, the labelled antibodies will be free to interact at the test line, producing a colour change that indicates a negative result. This format is particularly useful for smaller antigens that cannot accommodate multiple binding sites.

allergens [43]. In this format, as the analyte migrates across the membranes, it first interacts with the detection molecule (Fig. 3). This molecule should be very specific to the analyte of interest. Next, as this analyte-complex continues to move across the membrane, it interacts with another very specific 'capture' molecule that has been immobilised at the test line, building a sandwich: capture molecule—analyte—detection molecule. This creates a line of colour that can be seen with the naked eye, indicating a positive result. If there is no analyte in the sample, the capture molecule and detection molecule will not interact, and thus there will be no line of colour, indicating a negative result.

The home pregnancy test was the first commercial LFIA [44] and is the most common example of a sandwich assay. Here, antibodies are immobilised at the test line and also used as the detector molecule to detect human chorionic gonadotrophic (hCG) to predict pregnancy [45]. hCG is a hormone, usually only present in pregnant women, and is excreted in urine.

The competitive assay is sometimes referred to as an inhibition assay. It is normally reserved for analytes that are too small to have multiple binding sites. Common examples include drugs testing [46] and toxin testing [47–49]. In this format, there is not a capture molecule at the test line,

instead, synthetic target analyte is immobilised here (Fig. 3). As above, if the sample contains analyte of interest, it will first interact with a detector molecule at the conjugation pad, however, this complex will not interact at the test line. There will be no colour change, indicating a negative result. On the other hand, if there is no analyte of interest in the sample, the detector molecule will interact with the immobilised synthetic analyte at the test line, producing a line of colour, indicating a positive result.

Both the sandwich and competitive formats potentially allow for multiplexing multiple test lines into the paper strip to detect multiple different analytes [50–52]. This can be very useful in contaminant or toxin monitoring in food safety applications whereby simultaneous occurrence can occur and in the case of shellfish toxins as referenced prevents the need for three separate tests with three different sample preparation methods. Multiplexing can also be useful when multiple diseases that produce similar symptoms are endemic to the same region. For example, this is particularly useful for febrile illnesses such as dengue fever and yellow fever [53], as early identification can lead to timelier treatment. Due to the highly specific nature of antibodies, a multiplex LFIA can even distinguish between different variants of the same disease, such as different dengue serotypes [54]; this can be useful because different serotypes are associated with the severity of the disease [55]. That said, it can be very challenging to multiplex LFIAs and there are some key points to consider during development. For example, increasing the number of test zones on the membrane means that the test zones have to spaced more closely together or the test must be bigger [56]. In the first example, this can make it more difficult to distinguish between test lines, in the second example, this can increase test run time. Furthermore, due to the 2-dimensional nature of the LFIA, reactions occur in sequence. This means that the binding interactions at the first test line can subsequently interfere with downstream test lines by slowing the liquid flow across the membrane, or even blocking other antibody/analyte complexes from proceeding past. In this case, careful consideration must be given to the compatibility of different antigens on the same test, the order the lines are printed [57], or how the lines are printed [52].

No matter the format—sandwich, competitive, singleplex, or multiplex—there is always a control line that functions independently from the test line(s). Here, a capture molecule is immobilised that will detect a separate detection molecule—neither of which should interact with molecules found in the liquid sample. For example, Houghton et al. designed an LFIA to detect capsular polysaccharide in patient blood samples [58]. Here, they

used conjugated chicken antibodies in the conjugation pad, and anti-chicken antibodies at the control line—neither of which interacted with the many biological molecules found in human blood.

2.3 Microfluidic paper-based analytical devices (μPADs)

Microfluidic paper-based analytical devices (μPADs) further expands upon lateral flow technology. Like the LFD, μPADs rely on capillary action to move a sample across a series of membranes, however, these membranes are not always arranged linearly and there are often additional elements embedded into the device to manipulate the sample's pathing through the device for more complex reactions (Fig. 1C). Here, there are many different approaches. For example, one approach is '3D-printed' biosensors, whereby the paper membrane is printed with a hydrophobic substrate that produces channels that guide the liquid flow across the paper (Fig. 5A).

There are many different printing methods available, examples include: wax printing [59], inkjet printing [60], digital light processing (DLP) [61], photolithography [62], laser treatment [63], plasma processing [64], flexographic printing [65], and chemical vapour deposition [66]. In these examples, hydrophobic physical barriers are deposited onto a hydrophilic membrane to guide the liquid sample through a series of zones or areas. There are benefits and disadvantages for each method, usually centred around resolution and cost. For example, wax printing is inexpensive and uses a printer to deposit wax channels on paper, however this method is low resolution and can be inconsistent due to the way wax spreads on paper membranes [59]. Martinez et al. [62] describe the use of photolithography to print photoresist polymer channels on paper to measure glucose and BSA protein levels in urine; this method is fast, making it ideal for prototype testing. Additionally, it is high resolution, and can produce multiple millimetre-sized channels that only require a very small amount of sample to process (5 μL). On the downside, it has high equipment and material costs. Plasma processing is another high-resolution method. This method is unique in that the paper is rendered hydrophobic whilst hydrophilic channels are etched into the paper. This allows for highly complex patterns to be etched into the paper that allow for more complex fluid control, such as on-off flow switches [67] and fluid control channels [68]. That said, plasma etching is significantly more expensive than other methods.

Fluid does not only move horizontally; it can also move vertically. Another method for designing μPADs is '3D-folding', whereby the paper

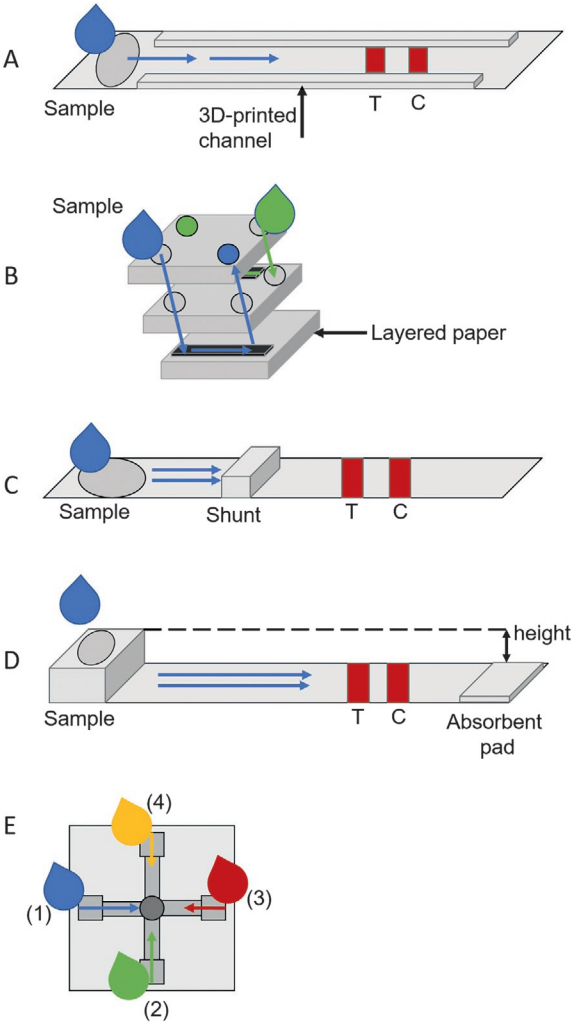

Fig. 5 Examples of Microfluidic paper-based analytical devices (μPADs). (A) '3D-printed' biosensors, are paper membranes printed with a hydrophobic substrate that produces channels to guide the liquid flow across the paper. The channels can be made from a variety of substrates, including wax or ink. (B) Some μPADs are designed in both the horizontal and vertical spaces. For example, a liquid sample can be diverted through layers of paper to increase the complexity of the sample's pathing allowing for more complicated biochemical reactions. (C) An absorbent shunt can be used to slow a liquid sample across a membrane. Upon encountering the shunt, the liquid will not be able to proceed until the shunt is completely saturated. (D) The difference in height between the inlet and outlet can alter the liquid sample's velocity via pressure. The greater the height difference, the greater the pressure difference, and the faster the liquid sample's velocity. (E) Surfactants can be impregnated into the membrane to alter or slow the liquid sample's velocity. This can allow multi-step reactions to occur in a controlled sequence.

membrane itself is layered or folded in such a way to control the sample's pathing (Fig. 5B). This can include using 3-dimensional geometrical patterns, layering different types of membrane together, and/or by altering the physical properties of the membrane. In a proof-of-concept study, Martinez et al. [69] fabricated a 3D paper-based biosensor by stacking layers of patterned paper with double sided sticky tape in a way that channelled the liquid within and between layers of paper. Here, a liquid sample could pass from a single inlet at the top of the device into multiple distinct outlets at the bottom of the device allowing the device to detect multiple analytes simultaneously. Liu and Crooks [70] expanded on this idea with a single sheet of photolithographic printed chromatography paper that could be folded, which they call the origami Pad (oPad); this method reduces production costs simplifies the device design as the output can be on any folded layer. Once the test is complete, the paper can be unfolded and the outputs read. A variety of 3D μPADs have since been developed, including devices to monitor glucose levels [71] and for malaria/dengue detection [72] and with new tests constantly being developed as proof of concepts.

Besides layering and folding, there are many additional techniques μPADs can implement to control fluid flow and pathing. These can range from the relatively simple, for example, narrowing or widening the membrane [73], to more complex methods incorporating additional materials into the μPAD; this can be physical or chemical additions that can slow the liquid sample's velocity, speed it up, or divert it into additional channels.

There are many ways to slow a liquid's velocity through a membrane. For example, a membrane shunt can be included in the fluid's path to slow the fluid's velocity [74] (Fig. 5C); liquid is absorbed into the shunt until saturation before being able to pass to the next zone of the test. Similarly, sucrose gradients can be used to slow the sample's pathing; Lutz et al. [75] described a method combining multiple sample paths of varying sucrose gradients to control the order in which reagents approach the detection zone; a sucrose gradient delays the fluid flow due to the dissolving time and by changing the liquid's viscosity. This allowed them to incorporate multiple wash steps and finally a gold enhancement reagent to improve the sensitivity of their malaria diagnostic biosensor. There are also approaches using pressure paper to restrict fluid movement and reduce velocity [76]. In this approach, by simply compressing parts of the membrane decreases pore size and permeability, thus decreasing the flow rate in the affected area. The amount of pressure applied changes the flow rate,

with more pressure meaning slower flow rates; this is another way to control multistep reactions [77].

On the other hand, pressure can also be used to increase a fluid's velocity through a membrane. In this approach, the pressure is not derived from physical interaction with the test, rather by the height difference between the inlet and outlet reservoirs [78]. In summary, the larger the height difference, the greater the pressure, and the faster the liquid's velocity (Fig. 5D). Another way to increase a fluid's velocity is to sandwich the paper membrane between two films: this can reduce evaporation and thus liquid velocity is increased [79]. Still another approach involves layering hollow tubes into the biosensor [80]; this can significantly increase velocity, reduce testing time, and has the additional benefit of allowing larger molecules to be transported, such as whole cells, that would not normally be able to pass through a membrane.

Alternatively, valves and polymers can be integrated to divert the sample's pathing. These can perform various functions, for example turn fluid flow off, turn it on, or divert it into multiple channels. Many types of valves have been developed and range from relatively simple to relatively complex. For example, dissolvable sucrose bridges can break the link between channels and prevent additional liquid from moving to the next area of the test [81]. Alternatively, Kong et al. [82] designed an actuator valve by folding chromatography paper; wetting of the valve causes the paper to unfurl and connect two channels. Using this method, they were able to design an autonomous colorimetric μPAD to detect three analytes in saliva. Similarly, expandable valves have been designed to expand when wet (like a sponge) and move the fluid to another channel [83].

Additionally, there are methods that alter the membrane itself, for example with surfactants. Here, dried surfactants are deposited into the μPAD channel; when the fluid interacts with them, the surfactant dissolves, increasing the surface tension in the region and slowing or preventing fluid flow [84,85] (Fig. 5E). There have been similar methods developed with hydrogels. For example, Wei et al. [86] used an aptamer-based hydrogel as a target-responsive flow regulator. Here, in the absence of a target, a hydrogel barrier forms in the μPAD channel that prevents an output signal from developing. If there is a target in the liquid sample, the aptamers preferentially bind to that; thus, no hydrogel is formed, and an output signal can develop. This approach is robust, even in complex biological matrices.

Regardless of the method, dipstick, LFD, or μPAD, they all function under the same overarching principles. In each method, biological and chemical reagents are deposited in discrete zones on the membrane, similar to a dipstick assay; the main benefit here is that multiple different reactions can be linked together in sequence. The format is very versatile and has been adapted for a variety of situations, such as: infectious disease diagnosis, cancer screening, glucose detection, environmental monitoring, and food safety tests.

3. Smartphones

Recently, smartphones have become ubiquitous. They are a necessary part of everyday life and are widely available across the world; current estimates predict that over 6.6 billion people have access to a smartphone as of February 2022 [87], roughly 82% of the global population. There are many companies that mass produce them, making them inexpensive. They continually get better each year. They have a plethora of features that come standard, such as a high-powered camera, large amounts of random access memory (RAM), and high-speed central processing units (CPUs) that can run complex analysis. Most smartphones also contain a global positioning system (GPS), can connect to Wi-Fi and cellular networks, and can download apps. Together, this means that diagnostic tests can be imaged, analysed, and results stored securely on-device, in the cloud, and also sent to additional stakeholders. Additionally, results can be tagged with appropriate metadata in real-time, such as time and location. These features are similar to and can even replace modern-day laboratory computers. For example, smartphones can be used as microscopes, spectrometers, luminometers, and colorimetric devices. Together, these features can help paper-based biosensors become truly integrated solutions [88].

3.1 Smartphone cameras

As described thus far, paper-based biosensors are qualitative or semi-quantitative; they rely on the naked eye to detect a colour change, which informs the result. Whilst this can be effective when the analyte is in excess or when quantification is unnecessary, there are many scenarios where it would be helpful to have a quantifiable result, for example when monitoring HIV titres during treatment. Additionally, results can be more difficult to interpret when approaching the limit of detection of the test; different people have different visual acuity which can affect how they interpret the results. Smartphone cameras can substantially expand the capabilities of

paper-based biosensors by capturing an image of the test zone. This image can then be sent to a qualified professional for additional interpretation [89], or in some cases analysed on device by an algorithm. This can help standardise results. That said, there are some key challenges.

First, image capture can be difficult. Smartphone cameras use complementary metal-oxide-semiconductor (CMOS) arrays, which integrate many functions that simplify photography for a more general consumer, such as auto-focusing, auto-exposure, and auto white balance (AWB). Some of these features can easily be disabled, however, for example, AWB can be difficult or impossible to disable. This feature automatically adjusts the Red, Green, Blue (RGB) signals at different ratios to brighten images and makes them more aesthetically pleasing. However, changing the RGB signal can disrupt the accuracy of a diagnostic test, especially when trying to analyse intensity for quantification [90]. Next, different ambient lighting conditions can affect the image quality. Everything absorbs light in a specific wavelength range whilst reflecting the rest; the smartphone camera is measuring the intensity of the reflected light. The intensity can change due to many variables, for example to the position of the light source, the light temperature, and where the picture is taken, e.g., indoors or outdoors. Similarly, even the angle the camera is held at can interfere with the quality of the results, by changing the reflectivity of the test device surface.

The best way to avoid this problem is to manually control all camera functions to ensure consistency between tests, and indeed, almost all commercially available tests to date do this, by providing their own camera reader devices (at an additional cost). The camera is normally enclosed in a light-shielding box, and tests are imaged inside the device to prevent ambient lighting distortions. However, this is not realistic in a resource-poor setting, where people are not likely to have access to these singular bespoke camera devices, and indeed it can be wasteful when most people already have a functioning camera device in their pocket. Here, there are two main approaches.

One approach uses image-processing algorithms to analyse the results; this method is called digital image calorimetry (DIC). Everything absorbs light in a specific wavelength range whilst reflecting the rest; when a reaction occurs at the test zone, the analyte-reagent complexes changes the absorbance and reflected intensity of the zone, typically over a wide range of wavelengths. The smartphone camera can measure these changes in intensity with RGB measurements, and these can be transformed to other colour spaces as needed, such as: CMYK (Cyan, Magenta, Yellow, Black), HSB (Hue, Saturation, Brightness), or CIE L*a*b* (CIELab) measurements (Fig. 6).

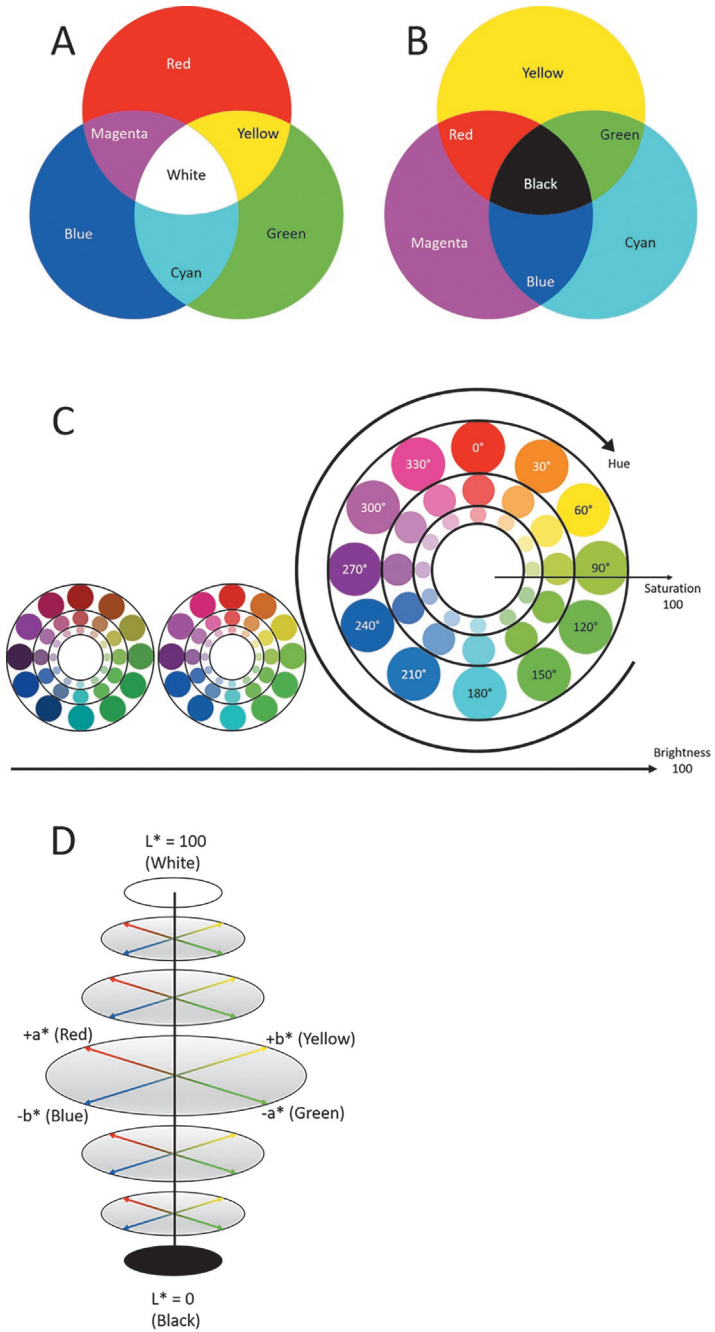

Fig. 6 Diagrams of various colour spaces. (A) Red, Green Blue (RGB). The RGB colour space is an additive model where colours are defined by how much red, green or blue

3.2 Red, green, blue (RGB)

The smartphone camera natively records red, green, and blue (RGB) measurements; thus, these are the most commonly used [91]. The RGB system is often represented on three axes', with each colour (Red, Green, or Blue) assigned to an XYZ axis with a scale from 0 to 256 (Fig. 6A). Along each axis, colour is represented by no contribution of that colour, some contribution of that colour, or full contribution by that colour. This is an additive model where colours are defined by how much red, green or blue is present. For example, pure red would be represented by the coordinates [256, 0, 0]. Pure blue would be represented as [0, 256, 0]. It is important to note that this is a non-uniform model. For example, Purple (a combination of red and blue), would be represented exactly between Red and Blue at [128, 128, 0]. However, this is not exactly how human vision recognises purple. It is also important to note that black is represented by [0, 0, 0] (the absence of all colours) whilst white is represented by [256, 256, 256] (max saturation of all colours).

Here, the smartphone cameras use a CMOS assay that assign a red, green, or blue value to each pixel photographed, and thus can measure broad colour shifts that occur at a test line. For example, Jalalvand et al. [32] describe RGB measurements to detect nitrate in food samples. Their platform is similar to the dipstick assay; a piece of Whatman filter paper is impregnated with Griess reagent and nitrate reductase. A liquid sample is placed on the paper: nitrate reductase converts any nitrates into nitrites, which interact with Griess reagents to produce a red coloured azo dye. The reaction is photographed with a smartphone and an algorithm calculates the concentration of nitrates in the sample based on the RGB colour intensities.

is present. (B) Cyan, Magenta, Yellow, Black (CMYK). The CMYK colour space a subtractive model that measures how much cyan, magenta, yellow, or black is present. (C) Hue, Saturation, Brightness (HSB). The HSB model neither additive nor subtractive; it is purely mathematical. Hue represents the colour on a 360° colour wheel, saturation is how injected in with colour it is (from 0% to 100%), whilst brightness is the intensity of reflected light (from 0% to 100%). (D) CIE L*a*b* (CIELab). CIELab is a system for defining colours in a plane that is closely aligned to how humans see colour. L* is luminance, how dark or bright the colour is, from 0 (black) to 100 (white). a* is the red to green coordinates, with +a* being more red and −a* being more green. b* represents the yellow to blue coordinates, where +b* is more yellow and −b* being more blue. Neutral grey occurs where the two colour axes intersect.

3.3 Cyan, magenta, yellow, and black (CMYK)

Other models may be more robust depending on the reaction at the test line, however, the RGB data must first be transformed with some mathematical model. For example, the CMYK colour space is very similar to the RGB colour space, except it measures Cyan, Magenta, Yellow, and Black (Fig. 6B). Importantly, this is a subtractive model, meaning White is set at [0, 0, 0] whilst Black is at [256, 256, 256]. Guo et al. [92] describe using a barcode assay for the detection and quantification of pesticides residues. Here, the reaction produced a yellow product inversely proportional to the amount of pesticide in the sample. Yellow and White overlap on the RBB matrix, thus will look similar, particularly low intensities of yellow could be miscategorised as white, so the signal was transformed to the CMYK model using app-based software. As the CMYK model is subtractive, White and Yellow do not overlap and thus are more easily distinguished.

3.4 Hue, saturation, brightness (HSB)

Another alternative to RGB measurements is HSB. This method defines colour space in 360 degrees based on 3 parameters, hue, saturation, and brightness. Hue is the colour type, such as red, green or blue, saturation is the intensity of the colour, and brightness is dark or light exists in the colour (Fig. 6C). HSB is neither additive nor subtractive, rather colours are defined mathematically. Most work done to date has centred around the hue value. For example, Cantrell et al. [93] report the hue value from smartphone-camera imaged membranes as a robust and sensitive method for quantifying bitonal results. Here, they have shown that the hue value is easy to obtain, sensitive, and stable; because there is only one variable being measured, small changes in the assay conditions, such as lighting, do not greatly change the results.

3.5 CIE L*a*b* (CIELab)

Whilst the methods described thus far are effective for a singular colour change, this can be more complicated when there is a wider range of colour changes available with differing colours indicating differing results. Yang et al. [94] describe a commercially urinalysis dipstick with 11 gradient tests; for example, pH can be measured, where pH5 is orange, pH7 is green, and pH9 is teal. Here, RGB measurements are less useful because the RGB matrix is non-uniform; the absolute distance between orange and green

on an RGB scale, including the gradients between, is not accurately represented for this purpose. To overcome this challenge, they wrote an algorithm to transform RGB values from a smartphone camera image to CIELab values to quantitatively or semi-quantitatively evaluate all 11 urinalysis dipstick tests.

CIELab is a system designed by the International Commission on Illumination (CIE) for defining colours in a plane that is very closely aligned to how humans see colour; in the current iteration, L* stands for luminance, a* represents the colour change from red to green, and b* represents the colour change from yellow to blue (CIE L*a*b* or CIELab) (Fig. 6D). Essentially, it is a system where each colour is defined by 2 coordinates, thus it is perpetually uniform [95]. This makes it useful for quantitative calculations where the colour change is more nuanced. That said, there is a risk of colour degradation from processing or transforming the image using a different model [96].

In these examples, the workflow includes photographing a colour reference chart to calibrate the smartphone camera before starting. It is important to note that different smartphone cameras have different CMOS arrays, and thus need to be calibrated separately. Even still, these algorithms can be incredibly useful for analysing the intensity of the colour change at the test line in order to correlate test results to the concentration of analyte in the sample. Indeed, DIC has been implemented for a variety of paper biosensors, including to quantify metals and heavy metals, herbicides, pesticides, antibiotics, toxins, biological targets, and infectious diseases.

3.6 Add-on devices

A second solution is the use of add-on equipment, for example: external light sources, lenses, filters, holders, and/or attached enclosures. There can be many benefits to using additional hardware with the smartphone camera. For example, filters can be used in conjunction with the smartphone camera to record enzymatic activities that would not normally be visible to the naked eye. These assays can be much more sensitive than traditional colorimetric assays. For example, a smartphone camera with the appropriate filters can detect light emitted upon the excitement and decay of target-fluorophore complexes. Here, the light is emitted across a narrow emission spectrum, amplifying the signal, and reducing the limit of detection. For example, Grawe et al. [97] developed a membrane-based biosensor that could detect Superfolder green fluorescent protein (sfGFP) as

an indirect reporter of mercury in drinking water. A second system was developed to detect sfGFP as an indirect reporter of gamma-butryic acid (GHB) the date rape drug. Uniquely, these systems use cell-free protein synthesis (CFPS) to link sfGFP concentrations to their respective analyte.

sfGFP is an ideal reporter for fluorescent detection because it folds rapidly, remains stable under harsh conditions, and small amounts are easy to detect [98], albeit not with the naked human eye nor with the standard smartphone CMOS array. To overcome this challenge, Graw et al. [97] used a two-filter system whereby one filter was placed in front of the flash and one filter was placed in front of the camera lenses. Here, the flash is used to excite the fluorophore, whilst the camera records the decay. Another challenge is that a dark environment is required for accurate fluorescence detection. Graw et al. [97] designed and produced a 3D-printed box to photograph the images inside. This device has the added benefit of automatically aligning the smartphone camera with the filters and the membrane, ensuring consistency and reproducibility between tests. In some sense this simplifies the process and helps overcome many of the challenges of using a smartphone camera as outlined above, albeit at an additional cost and reduced accessibility.

3.7 Digital connectivity

Smartphones can enhance paper-based biosensors via their ability to connect to Wi-Fi and cellular networks. This has many benefits for the user. For example, as described, because paper-based biosensors are user-friendly, inexpensive, lightweight, and portable, they are primarily used in a decentralised manner: at home, on-site or in the field. However, even though they are user-friendly, the end-user can still intentionally or unintentionally make mistakes. Here, having connectivity allows for image- or video-based telemedicine; a professional to video call the user, explain the procedure, and then monitor for compliance. This can be particularly helpful to reduce the spread of disease and limit risk to healthcare providers, as they do not have to be in physical proximity to those being tested. For example, this method was used extensively during the covid-19 pandemic, where healthcare providers could certify that people were administering self-tests appropriately to reduce the spread of SARS-CoV-2, for example during air travel [99,100]. Here, it is important to make sure those being tested have access to adequate support, especially in the advent of a positive result. Whilst telemedicine in

this way can improve accessibility to healthcare, it can also be isolating and worrying, particularly when the result can be life changing.

After administering the test, the results can be securely uploaded to the cloud for backup and also for instant sharing with key stakeholders that can help interpret results, offer advice, and/or use the data as a part of wider research efforts. Furthermore, results can be interpreted based on historical data and with other metadata in mind, such as the time, date, and location where the test was performed. For example, Matthews et al. [101] developed a smartphone system for detection and notification of dengue fever. Here, if infection is suspected, patients can be administered a diagnostic μPAD. As in other described tests, results are photographed, and an on-device algorithm analyses the colour change at the test line to report if the patient is infected or not. Additionally, results are uploaded to the United States Center for Disease Control (CDC) for further analysis and uploaded to a web server to provide healthcare providers with up-to-date spatial information on outbreaks.

3.8 Additional tools

More recently, some paper-based biosensors have also begun integrating electronic components to improve sensitivity of the test and increase the limit of detection. In their seminal work, Dungchai et al. [102] developed the first electrochemical paper-based biosensor; it can monitor levels of glucose, lactate, and uric acid in biological samples. Photolithography was used to make microfluidic channels into filter paper, and screen-printing was utilised to integrate electrodes directly onto the device. Glucose, lactate, and uric acid are detected with oxidase enzyme reactions and an external potentiometric device. More recently, potentiometric devices have been integrated with the smartphone, for example through the audio jack [103,104], through USB [105], or through Bluetooth [106]; this reduces the cost, increases portability, and allows the user to benefit from all of the aforementioned digital connectivity advantages a smartphone provides.

3.9 Challenges

It is a very exciting time, with improvements constantly being made and a seemingly never-ending research and development pipeline. That said, it is important to remember that whilst smartphones seem ubiquitous, there is still much work to be done before they become ubiquitous as companion diagnostic devices.

3.9.1 Technical limitations

Smartphones are produced by a variety of manufacturers and operate a variety of mobile operating systems. Android and iOS are currently the dominant operating systems, however, there are still many smartphones in circulation that use other systems, for example Windows Phone, BlackBerry 10, Symbian, and Tizen. Some of these are no longer being developed or supported, for example Windows Phone was discontinued in 2020 after just 10 years in circulation [107]. Similarly, the Blackberry 10 OS was discontinued after just 7 years in use [108]. Herein lies the first challenge: diagnostics developers do not have control over the smartphone platform. If the operating system stops being supported, this can cause the underlying coding and application programming interfaces (APIs) to stop working, rendering the device useless for its diagnostic intentions. Indeed, even working with the dominant operating systems comes with risk: Apple (iOS) and Alphabet (Android) release yearly updates to their operating systems that change different APIs. This means applications must be regularly supported and updated to continue to work.

Next, there are a plethora of smartphone manufacturers that all use differing hardware. As previously discussed, this can cause obvious problems for imaging, as different smartphone camera CMOS arrays do not always take comparable images. But different smartphones also have differing levels of random-access memory (RAM) and central processing units (CPU) which may limit their processing powers. Some of the tests discussed utilised audio jacks or Bluetooth to transfer data, but here again, not all smartphones have audio jacks and there are multiple differing Bluetooth standards available. Additionally, Wi-Fi and cellular network standards are constantly evolving, with older network technologies being discontinued. For example, many mobile phone operators in the USA are shutting down their 3G networks, meaning phones that depend on 3G connectivity will no longer be able to connect to the internet and users will need to purchase a new device.

Software and hardware updates not only bring out new features and APIs, but they also update security protocols. If devices are not updated or if suppliers continue to rely on outdated hardware or unsupported operating systems, they risk being open to security vulnerabilities and privacy violations. This can have serious legal ramifications, especially when processing sensitive health information.

3.9.2 Regulatory compliance

Together, these can feed into difficulties maintaining regulatory compliance, especially when used as a diagnostic medical device. In every region, medical

devices must comply with safety and efficacy regulations because these devices can strongly influence personal health. For example, diabetic patients must monitor their blood glucose levels to help make diet and medication dosing decisions; currently, this is often done with an LFD and a handheld reader [109]. That said, these devices can also strongly influence public health. For example, biosensors measuring the concentration of algal toxins in shellfish [47–49] can influence whether a grower harvests and distributes their catch; here, inaccuracies could result in contaminated stock being consumed by the general public. Similarly, LFDs were widely used to inform people if they needed to self-isolate to prevent the spread SARS-CoV-2 pandemic [110]; inaccuracies here could cause further spread of disease.

The path to regulatory approval is complicated, different depending on the category of device, and different in different regions; see Gupta (2015) [111] for a comprehensive list of medical device regulatory bodies and laws by country or region. Medical device regulatory bodies usually require pre-market and post-market surveillance [111]. Pre-market surveillance includes research data demonstrating safety and effectiveness, essentially, showing that the device is safe to use and will not harm users when using it or, for example, by providing unreliable diagnostic results. On the other hand, post-market surveillance involves monitoring the device whilst it is actively being used in real-world situations. Specifically, regulatory bodies are looking at device-related malfunctions, injuries, or death caused by the device or caused by unreliable diagnostic readings.

Many countries use a 3-tier or a 4-tier risk-based system for classifying medical devices [111]. Lower class devices are least likely to cause harm to a patient or user, whilst higher classes can have a much higher risk on malfunction or even be life-sustaining devices. For example, the Food and Drug Administration (FDA) oversees the marketing of medical devices in the United States [112]. Here, a 3-tiered risk-based system is used where Class I is the lowest risk, Class II has intermediate risk, and Class III has the highest risk. Most paper-based biosensors are considered Class II devices. This means they must be approved by the FDA before they are launched, however, assessment can come in the form of laboratory research or animal testing and does not necessarily require clinical testing [113]. An example of a Class I device would be an elastic bandage, whereas an example of a Class III device is a pacemaker.

Regulatory approval in one country does not always guarantee approval in another country. For example, the European Union places in vitro diagnostics into their own distinct category, separate from medical devices [114].

Here, they are still classified into four risk-based tiers: A (low risk), B (moderate risk), C (high risk for individual patients) and D (high public health risk). These tiers are dependent on the function of the test [115]. For example, a cholesterol self-testing would be considered Class B as the results will only affect the patient and are not immediately life-threatening. On the other hand, an infectious disease diagnostic test could be considered Class D because the results will not only affect the patient, but could also impact the spread of disease to others. Each member state is responsible for nominating its own competent authorities to approve the diagnostic test.

That said, not all paper-based biosensors are medical devices; there are many other uses, including food safety and environmental sampling. In the United States these categories of test still fall under the FDA's remit for regulatory approval, however, in other countries, there may be separate legislation responsible for approving non-medical biosensors. For example, in the European Union, Commission Regulation (EU) No. 853/2004 stipulates the specific hygiene and testing standards for monitoring marine toxins in shellfish [116], whilst Commission Regulation (EU) No. 519/2014 stipulates the requirements for mycotoxin testing in food supplements [117]; in the United Kingdom, these are overseen by the Food Standards Agency [118]. These regulations also stipulate the regulatory methods of analysis mainly as complicated high performance liquid chromatography and mass spectrometry-based methods. However, the production industry is in desperate need of portable tools for in field testing for product release systems as the turnaround time of these regulatory methods can be detrimental to their industry in an ever-changing tidal environment. Lateral flow immunoassays are available commercially [119] and are also now being considered in different parts of the world as regulatory tools for shellfish toxin analysis or as part of end product release systems for shellfish harvest [120]. Some of these devices are already available and used in tandem with reader devices for the three main groups of toxins [47–49] and in development as multiplex tools [51], but the added immediate connectivity a smartphone could offer could be beneficial in a harvesting season for predictive monitoring in a network.

It is important to remember that regulatory approval extends to both the biosensor, and also to any adjunct device or software, for example, if using the biosensor in conjunction with a smartphone camera and smartphone application. This can be tricky as mobile operating system updates and applications updates can outpace approval processes [121,122].

4. Looking ahead

Paper-based biosensors are becoming increasingly popular due to their versatility. From the humble dipstick assay to much more complex μPADs, paper-based biosensors have the opportunity to make diagnostic testing more equitable and accessible, especially in resource-poor settings. They are lightweight and small in size, making them easily portable. They are robust and inexpensive to produce with biodegradable materials and they can accommodate an incredibly diverse range of sample types and applications, including clinical diagnostics, veterinary diagnostics, food safety sampling, and environmental sampling. More recently, the smartphone has been identified as adjunct to make these devices even more compelling. Smartphones can improve connectivity, helping users administer their test properly and understand their results. They can help key stakeholders monitor results remotely across large populations, for example, to better understand the spread of disease. Additionally, smartphone cameras can improve imaging and allow for even more sensitive testing strategies. These benefits come with minimal additional costs, as smartphones are ubiquitous devices that large swathes of the global population already have in their pockets. Going forward, there will be some key challenges to ensure compatibility between smartphones, support for legacy devices, ensuring regulatory compliance across regions, and maintaining pace with operating system upgrades and application update versions. However, as we have observed, paper-based biosensors have come a long way since their early designs. They are proven to be robust and relatively reliable diagnostic test kits, and there is no doubt they will continue to thrive and adapt into the future.

References

[1] M. Liu, S. Suo, J. Wu, Y. Gan, H. AHD, C.Q. Chen, Tailoring porous media for controllable capillary flow, J. Colloid Interface Sci. 539 (2019) 379–387. Available from: https://doi.org/10.1016/j.jcis.2018.12.068.

[2] A. Mishra, S. Patra, V. Srivastava, L. Uzun, Y.K. Mishra, M. Syväjärvi, et al., Progress in paper-based analytical devices for climate neutral biosensing, Biosens. Bioelectron. X 11 (2022), 100166. Available from https://linkinghub.elsevier.com/retrieve/pii/S2590137022000619.

[3] R.W. Peeling, D. Mabey, Point-of-care tests for diagnosing infections in the developing world, Clin. Microbiol. Infect. 16 (2010) 1062–1069. Available from https://linkinghub.elsevier.com/retrieve/pii/S1198743X14641951.

[4] L.S. Foster, I.J. Gruntfest, Demonstration experiments using universal indicators, J. Chem. Educ. 14 (1937) 274. Available from https://pubs.acs.org/doi/abs/10.1021/ed014p274.
[5] C.A. Chukwu, A. Rao, P.A. Kalra, R. Middleton, Managing recurrent urinary tract infections in kidney transplant recipients using smartphone assisted urinalysis test, J. Ren. Care 48 (2022) 119–127. Available from https://onlinelibrary.wiley.com/doi/10.1111/jorc.12405.
[6] P. Griess, Vorläufige Notiz über die Einwirkung von salpetriger Säure auf Amidinitro- und Aminitrophenylsäure (Preliminary notice of the reaction of nitrous acid with picramic acid and aminonitrophenol), Ann. Chem. Pharm. 106 (1858) 123–125.
[7] V.T. Andriole, Urinary tract infections: recent developments, J. Infect. Dis. 156 (1987) 865–869. Available from https://academic.oup.com/jid/article-lookup/doi/10.1093/infdis/156.6.865.
[8] E.G. Welles, E.M. Whatley, A.S. Hall, J.C. Wright, Comparison of multistix PRO dipsticks with other biochemical assays for determining urine protein (UP), urine creatinine (UC), and UP:UC ratio in dogs and cats, Vet. Clin. Pathol. 35 (2006) 31–36. Available from https://onlinelibrary.wiley.com/doi/10.1111/j.1939-165X.2006.tb00085.x.
[9] M. Pohanka, J.Z. Karasova, K. Kuca, J. Pikula, O. Holas, J. Korabecny, et al., Colorimetric dipstick for assay of organophosphate pesticides and nerve agents represented by paraoxon, sarin and VX, Talanta 81 (2010) 621–624. Available from: https://doi.org/10.1016/j.talanta.2009.12.052.
[10] H.Y. No, Y.A. Kim, Y.T. Lee, H.S. Lee, Cholinesterase-based dipstick assay for the detection of organophosphate and carbamate pesticides, Anal. Chim. Acta 594 (2007) 37–43. Available from https://linkinghub.elsevier.com/retrieve/pii/S0003267007008586.
[11] S.A. Frank, Immunology and Evolution of Infectious Disease, Princeton University Press, Princeton, New Jersey, 2002.
[12] G. Köhler, C. Milstein, Continuous cultures of fused cells secreting antibody of predefined specificity, Nature 256 (1975) 495–497. Available from http://www.nature.com/articles/256495a0.
[13] V. Marx, Finding the right antibody for the job, Nat. Methods 10 (2013) 703–707. Available from: http://www.nature.com/articles/nmeth.2570.
[14] J. Bordeaux, A.W. Welsh, S. Agarwal, E. Killiam, M.T. Baquero, J.A. Hanna, et al., Antibody validation, Biotechniques 48 (2010) 197–209. Available from https://www.future-science.com/doi/10.2144/000113382.
[15] C. Tuerk, L. Gold, Systematic evolution of ligands by exponential enrichment: RNA ligands to bacteriophage T4 DNA polymerase, Science 249 (1990) 505–510. Available from: https://www.science.org/doi/10.1126/science.2200121.
[16] A.D. Ellington, J.W. Szostak, In vitro selection of RNA molecules that bind specific ligands, Nature 346 (1990) 818–822. Available from http://www.nature.com/articles/346818a0.
[17] S.C.B. Gopinath, Methods developed for SELEX, Anal. Bioanal. Chem. 387 (2007) 171–182. Available from https://link.springer.com/10.1007/s00216-006-0826-2.
[18] Z. Zhu, Y. Song, C. Li, Y. Zou, L. Zhu, Y. An, et al., Monoclonal surface display SELEX for simple, rapid, efficient, and cost-effective aptamer enrichment and identification, Anal. Chem. 86 (2014) 5881–5888. Available from https://pubs.acs.org/doi/10.1021/ac501423g.
[19] T. Schütze, P.F. Arndt, M. Menger, A. Wochner, M. Vingron, V.A. Erdmann, et al., A calibrated diversity assay for nucleic acid libraries using DiStRO—a diversity standard of random oligonucleotides, Nucleic Acids Res. 38 (2010) e23. Available from https://academic.oup.com/nar/article-lookup/doi/10.1093/nar/gkp1108.

[20] S. Hoon, B. Zhou, K.D. Janda, S. Brenner, J. Scolnick, Aptamer selection by high-throughput sequencing and informatic analysis, Biotechniques 51 (2011) 413–416. Available from https://www.future-science.com/doi/10.2144/000113786.
[21] S. Tsuji, N. Hirabayashi, S. Kato, J. Akitomi, H. Egashira, T. Tanaka, et al., Effective isolation of RNA aptamer through suppression of PCR bias, Biochem. Biophys. Res. Commun. 386 (2009) 223–226. Available from: https://doi.org/10.1016/j.bbrc.2009.06.013.
[22] H. Sun, Y. Zu, A highlight of recent advances in aptamer technology and its application, Molecules 20 (2015) 11959–11980. Available from http://www.mdpi.com/1420-3049/20/7/11959.
[23] C. Seidel, S. Peters, E. Eschbach, A.T. Feßler, B. Oberheitmann, S. Schwarz, Development of a nucleic acid lateral flow immunoassay (NALFIA) for reliable, simple and rapid detection of the methicillin resistance genes mecA and mecC, Vet. Microbiol. 200 (2017) 101–106. Available from: https://doi.org/10.1016/j.vetmic.2016.08.009.
[24] S. Pecchia, D. Da Lio, Development of a rapid PCR-nucleic acid lateral flow immunoassay (PCR-NALFIA) based on rDNA IGS sequence analysis for the detection of Macrophomina phaseolina in soil, J. Microbiol. Methods 151 (2018) 118–128. Available from: https://doi.org/10.1016/j.mimet.2018.06.010.
[25] X. Mao, W. Wang, T.E. Du, Dry-reagent nucleic acid biosensor based on blue dye doped latex beads and lateral flow strip, Talanta 114 (2013) 248–253. Available from: https://doi.org/10.1016/j.talanta.2013.04.044.
[26] M. Blažková, B. Mičková-Holubová, P. Rauch, L. Fukal, Immunochromatographic colloidal carbon-based assay for detection of methiocarb in surface water, Biosens. Bioelectron. 25 (2009) 753–758.
[27] M. Blažková, P. Rauch, L. Fukal, Strip-based immunoassay for rapid detection of thiabendazole, Biosens. Bioelectron. 25 (2010) 2122–2128.
[28] C. Suárez-Pantaleón, J. Wichers, A. Abad-Somovilla, A. Van Amerongen, A. Abad-Fuentes, Development of an immunochromatographic assay based on carbon nanoparticles for the determination of the phytoregulator forchlorfenuron, Biosens. Bioelectron. 42 (2013) 170–176.
[29] W. Qiu, H. Xu, S. Takalkar, A.S. Gurung, B. Liu, Y. Zheng, et al., Carbon nanotube-based lateral flow biosensor for sensitive and rapid detection of DNA sequence, Biosens. Bioelectron. 64 (2015) 367–372. Available from: https://doi.org/10.1016/j.bios.2014.09.028.
[30] A.N. Kawde, X. Mao, H. Xu, Q. Zeng, Y. He, G. Liu, Moving enzyme-linked immunosorbent assay to the point-of-care dry-reagent strip biosensors, Am. J. Biomed. Sci. 2 (2010) 23–32. Available from http://www.nwpii.com/ajbms/papers/AJBMS_2010_1_03.pdf.
[31] Z. Urusov, Dzantiev., Towards lateral flow quantitative assays: detection approaches, Biosensors 9 (2019) 89. Available from: https://www.mdpi.com/2079-6374/9/3/89.
[32] A.R. Jalalvand, M. Mahmoudi, H.C. Goicoechea, Developing a novel paper-based enzymatic biosensor assisted by digital image processing and first-order multivariate calibration for rapid determination of nitrate in food samples, RSC Adv. 8 (2018) 23411–23420.
[33] N. Mohamad Nor, K. Abdul Razak, S.C. Tan, R. Noordin, Properties of surface functionalized iron oxide nanoparticles (ferrofluid) conjugated antibody for lateral flow immunoassay application, J. Alloys Compd. 538 (2012) 100–106. Available from: https://doi.org/10.1016/j.jallcom.2012.05.053.
[34] Y. Wang, H. Xu, M. Wei, H. Gu, Q. Xu, W. Zhu, Study of superparamagnetic nanoparticles as labels in the quantitative lateral flow immunoassay, Mater. Sci. Eng. C 29 (2009) 714–718. Available from: https://doi.org/10.1016/j.msec.2009.01.011.

[35] Z. Li, Y. Wang, J. Wang, Z. Tang, J.G. Pounds, Y. Lin, Rapid and sensitive detection of protein biomarker using a portable fluorescence biosensor based on quantum dots and a lateral flow test strip, Anal. Chem. 82 (2010) 7008–7014. Available from https://pubs.acs.org/doi/10.1021/ac101405a.
[36] J.K. Jaiswal, S.M. Simon, Potentials and pitfalls of fluorescent quantum dots for biological imaging, Trends Cell Biol. 14 (2004) 497–504.
[37] J.M. Costa-Fernández, R. Pereiro, A. Sanz-Medel, The use of luminescent quantum dots for optical sensing, TrAC Trends Anal. Chem. 25 (2006) 207–218. Available from https://linkinghub.elsevier.com/retrieve/pii/S0165993605002062.
[38] F. Zhang, M. Zou, Y. Chen, J. Li, Y. Wang, X. Qi, et al., Lanthanide-labeled immunochromatographic strips for the rapid detection of Pantoea stewartii subsp. Stewartii, Biosens. Bioelectron. 51 (2014) 29–35. Available from: https://doi.org/10.1016/j.bios.2013.06.065.
[39] P. Wang, R. Wang, W. Zhang, X. Su, H. Luo, Novel fabrication of immunochromatographic assay based on up conversion phosphors for sensitive detection of clenbuterol, Biosens. Bioelectron. 77 (2016) 866–870. Available from https://linkinghub.elsevier.com/retrieve/pii/S0956566315305157.
[40] J.S. Ahn, S. Choi, S.H. Jang, H.J. Chang, J.H. Kim, K.B. Nahm, et al., Development of a point-of-care assay system for high-sensitivity C-reactive protein in whole blood, Clin. Chim. Acta 332 (2003) 51–59. Available from https://linkinghub.elsevier.com/retrieve/pii/S000989810300113X.
[41] Y. Sbihi, N. El Abbadi, A. Iddar, Lateral flow immunogold assay as a rapid detection tool for screening of congenital hypothyroidism, J. Immunoass. Immunochem. 42 (2021) 393–405. Available from: https://doi.org/10.1080/15321819.2021.1891931.
[42] L.F. Yang, N. Kacherovsky, N. Panpradist, R. Wan, J. Liang, B. Zhang, et al., Aptamer sandwich lateral flow assay (aptaflow) for antibody-free SARS-CoV-2 detection, Anal. Chem. 94 (2022) 7278–7285. Available from https://pubs.acs.org/doi/10.1021/acs.analchem.2c00554.
[43] A. Civera, P. Galan-Malo, I. Segura-Gil, L. Mata, A.P. Tobajas, L. Sánchez, et al., Development of sandwich ELISA and lateral flow immunoassay to detect almond in processed food, Food Chem. 371 (2022), 131338. Available from https://linkinghub.elsevier.com/retrieve/pii/S030881462102344X.
[44] W.C. Mak, V. Beni, A.P.F. Turner, Lateral-flow technology: from visual to instrumental, Trends Anal. Chem. 79 (2016) 297–305. Available from: https://doi.org/10.1016/j.trac.2015.10.017.
[45] C.M. Sturgeon, E.J. McAllister, Analysis of hCG: clinical applications and assay requirements, Ann. Clin. Biochem. Int. J. Lab. Med. 35 (1998) 460–491. Available from http://journals.sagepub.com/doi/10.1177/000456329803500402.
[46] M. Hudson, T. Stuchinskaya, S. Ramma, J. Patel, C. Sievers, S. Goetz, et al., Drug screening using the sweat of a fingerprint: lateral flow detection of Δ9-tetrahydrocannabinol, cocaine, opiates and amphetamine, J. Anal. Toxicol. 43 (2019) 88–95. Available from https://academic.oup.com/jat/article/43/2/88/5112962.
[47] W. Jawaid, K. Campbell, K. Melville, S.J. Holmes, J. Rice, C.T. Elliott, Development and validation of a novel lateral flow immunoassay (LFIA) for the rapid screening of paralytic shellfish toxins (PSTs) from shellfish extracts, Anal. Chem. 87 (2015) 5324–5332.
[48] W. Jawaid, J. Meneely, K. Campbell, M. Hooper, K. Melville, S. Holmes, et al., Development and validation of the first high performance-lateral flow immunoassay (HP-LFIA) for the rapid screening of domoic acid from shellfish extracts, Talanta 116 (2013) 663–669. Available from: https://doi.org/10.1016/j.talanta.2013.07.027.

[49] W. Jawaid, J.P. Meneely, K. Campbell, K. Melville, S.J. Holmes, J. Rice, et al., Development and validation of a lateral flow immunoassay for the rapid screening of okadaic acid and all dinophysis toxins from shellfish extracts, J. Agric. Food Chem. 63 (2015) 8574–8583.
[50] L. Anfossi, F. Di Nardo, S. Cavalera, C. Giovannoli, C. Baggiani, Multiplex lateral flow immunoassay: an overview of strategies towards high-throughput point-of-need testing, Biosensors 9 (2018) 2. Available from http://www.mdpi.com/2079-6374/9/1/2.
[51] C. Mills, M.J. Dillon, P.K. Kulabhusan, D. Senovilla-Herrero, K. Campbell, Multiplex lateral flow assay and the sample preparation method for the simultaneous detection of three marine toxins, Environ. Sci. Technol. (2022). Available from: https://pubs.acs.org/doi/10.1021/acs.est.2c02339.
[52] I.V. Safenkova, G.K. Pankratova, I.A. Zaitsev, Y.A. Varitsev, Y.Y. Vengerov, A.V. Zherdev, et al., Multiarray on a test strip (MATS): rapid multiplex immunodetection of priority potato pathogens, Anal. Bioanal. Chem. 408 (2016) 6009–6017. Available from http://link.springer.com/10.1007/s00216-016-9463-6.
[53] C.W. Yen, H. de Puig, J.O. Tam, J. Gómez-Márquez, I. Bosch, K. Hamad-Schifferli, et al., Multicolored silver nanoparticles for multiplexed disease diagnostics: distinguishing dengue, yellow fever, and Ebola viruses, Lab Chip 15 (2015) 1638–1641. Available from http://xlink.rsc.org/?DOI=C5LC00055F.
[54] S.C. Lai, Y.Y. Huang, J.J. Wey, M.H. Tsai, Y.L. Chen, P.Y. Shu, et al., Development of novel dengue NS1 multiplex lateral flow immunoassay to differentiate serotypes in serum of acute phase patients and infected mosquitoes, Front. Immunol. 13 (2022) 1–15. Available from https://www.frontiersin.org/articles/10.3389/fimmu.2022.852452/full.
[55] C.F. Yung, K.S. Lee, T.L. Thein, L.K. Tan, V.C. Gan, J.G.X. Wong, et al., Dengue serotype-specific differences in clinical manifestation, laboratory parameters and risk of severe disease in adults, Singapore, Am. J. Trop. Med. Hyg. 92 (2015) 999–1005. Available from https://ajtmh.org/doi/10.4269/ajtmh.14-0628.
[56] J. Li, J. Macdonald, Multiplexed lateral flow biosensors: technological advances for radically improving point-of-care diagnoses, Biosens. Bioelectron. 83 (2016) 177–192. Available from: https://doi.org/10.1016/j.bios.2016.04.021.
[57] A.V. Bartosh, D.V. Sotnikov, O.D. Hendrickson, A.V. Zherdev, B.B. Dzantiev, Design of multiplex lateral flow tests: a case study for simultaneous detection of three antibiotics, Biosensors 10 (2020) 17.
[58] R.L. Houghton, D.E. Reed, M.A. Hubbard, M.J. Dillon, H. Chen, B.J. Currie, et al., Development of a prototype lateral flow immunoassay (LFI) for the rapid diagnosis of melioidosis, PLoS Negl. Trop. Dis. 8 (2014), e2727. Available from https://dx.plos.org/10.1371/journal.pntd.0002727.
[59] E. Carrilho, A.W. Martinez, G.M. Whitesides, Understanding wax printing: a simple micropatterning process for paper-based microfluidics, Anal. Chem. 81 (2009) 7091–7095.
[60] K. Yamada, T.G. Henares, K. Suzuki, D. Citterio, Paper-based inkjet-printed microfluidic analytical devices, Angew. Chem. Int. Ed. 54 (2015) 5294–5310. Available from https://onlinelibrary.wiley.com/doi/10.1002/anie.201411508.
[61] C. Park, Y.D. Han, H.V. Kim, J. Lee, H.C. Yoon, S. Park, Double-sided 3D printing on paper towards mass production of three-dimensional paper-based microfluidic analytical devices (3D-μPADs), Lab Chip 18 (2018) 1533–1538. Available from http://xlink.rsc.org/?DOI=C8LC00367J.
[62] A.W. Martinez, S.T. Phillips, M.J. Butte, G.M. Whitesides, Patterned paper as a platform for inexpensive, low-volume, portable bioassays, Angew. Chem. Int. Ed. 46 (2007) 1318–1320.

[63] G. Chitnis, Z. Ding, C.L. Chang, C.A. Savran, B. Ziaie, Laser-treated hydrophobic paper: an inexpensive microfluidic platform, Lab Chip 11 (2011) 1161. Available from http://xlink.rsc.org/?DOI=c0lc00512f.
[64] C. Yan, S. Yu, Y. Jiang, Q. He, H. Chen, Fabrication of paper-based microfluidic devices by plasma treatment and its application in glucose determination, Acta Chim. Sin. 72 (2014) 1099. Available from http://sioc-journal.cn/Jwk_hxxb/CN/abstract/abstract344584.shtml.
[65] J. Olkkonen, K. Lehtinen, T. Erho, Flexographically printed fluidic structures in paper, Anal. Chem. 82 (2010) 10246–10250. Available from https://pubs.acs.org/doi/10.1021/ac1027066.
[66] B. Chen, P. Kwong, M. Gupta, Patterned fluoropolymer barriers for containment of organic solvents within paper-based microfluidic devices, ACS Appl. Mater. Interfaces 5 (2013) 12701–12707. Available from https://pubs.acs.org/doi/10.1021/am404049x.
[67] X. Li, J. Tian, T. Nguyen, W. Shen, Paper-based microfluidic devices by plasma treatment, Anal. Chem. 80 (2008) 9131–9134.
[68] N. Raj, V. Breedveld, D.W. Hess, Flow control in fully enclosed microfluidics paper based analytical devices using plasma processes, Sensors Actuators B Chem. 320 (2020) 128606.
[69] A.W. Martinez, S.T. Phillips, G.M. Whitesides, Three-dimensional microfluidic devices fabricated in layered paper and tape, Proc. Natl. Acad. Sci. 105 (2008) 19606–19611. Available from https://pnas.org/doi/full/10.1073/pnas.0810903105.
[70] H. Liu, R.M. Crooks, Three-dimensional paper microfluidic devices assembled using the principles of origami, J. Am. Chem. Soc. 133 (2011) 17564–17566.
[71] G.G. Morbioli, T. Mazzu-Nascimento, L.A. Milan, A.M. Stockton, E. Carrilho, Improving sample distribution homogeneity in three-dimensional microfluidic paper-based analytical devices by rational device design, Anal. Chem. 89 (2017) 4786–4792. Available from https://pubs.acs.org/doi/10.1021/acs.analchem.6b04953.
[72] R.N. Deraney, C.R. Mace, J.P. Rolland, J.E. Schonhorn, Multiplexed, patterned-paper immunoassay for detection of malaria and dengue fever, Anal. Chem. 88 (2016) 6161–6165. Available from https://pubs.acs.org/doi/10.1021/acs.analchem.6b00854.
[73] E. Fu, C. Downs, Progress in the development and integration of fluid flow control tools in paper microfluidics, Lab Chip 17 (2017) 614–628.
[74] B.J. Toley, B. McKenzie, T. Liang, J.R. Buser, P. Yager, E. Fu, Tunable-delay shunts for paper microfluidic devices, Anal. Chem. 85 (2013) 11545–11552. Available from https://pubs.acs.org/doi/10.1021/ac4030939.
[75] B. Lutz, T. Liang, E. Fu, S. Ramachandran, P. Kauffman, P. Yager, Dissolvable fluidic time delays for programming multi-step assays in instrument-free paper diagnostics, Lab Chip 13 (2013) 2840. Available from http://xlink.rsc.org/?DOI=c3lc50178g.
[76] J.H. Shin, J. Park, S.H. Kim, J.K. Park, Programmed sample delivery on a pressurized paper, Biomicrofluidics 8 (2014) 054121. Available from http://aip.scitation.org/doi/10.1063/1.4899773.
[77] J. Park, J.K. Park, Pressed region integrated 3D paper-based microfluidic device that enables vertical flow multistep assays for the detection of C-reactive protein based on programmed reagent loading, Sensors Actuators B Chem. 246 (2017) 1049–1055. Available from: https://doi.org/10.1016/j.snb.2017.02.150.
[78] J.H. Shin, G.J. Lee, W. Kim, S. Choi, A stand-alone pressure-driven 3D microfluidic chemical sensing analytic device, Sensors Actuators B Chem. 230 (2016) 380–387. Available from: https://doi.org/10.1016/j.snb.2016.02.085.
[79] S. Jahanshahi-Anbuhi, P. Chavan, C. Sicard, V. Leung, S.M.Z. Hossain, R. Pelton, et al., Creating fast flow channels in paper fluidic devices to control timing of sequential reactions, Lab Chip 12 (2012) 5079. Available from http://xlink.rsc.org/?DOI=c2lc41005b.

[80] C. Renault, X. Li, S.E. Fosdick, R.M. Crooks, Hollow-channel paper analytical devices, Anal. Chem. 85 (2013) 7976–7979.
[81] J. Houghtaling, T. Liang, G. Thiessen, E. Fu, Dissolvable bridges for manipulating fluid volumes in paper networks, Anal. Chem. 85 (2013) 11201–11204. Available from https://pubs.acs.org/doi/10.1021/ac4022677.
[82] T. Kong, S. Flanigan, M. Weinstein, U. Kalwa, C. Legner, S. Pandey, A fast, reconfigurable flow switch for paper microfluidics based on selective wetting of folded paper actuator strips, Lab Chip 17 (2017) 3621–3633.
[83] B.J. Toley, J.A. Wang, M. Gupta, J.R. Buser, L.K. Lafleur, B.R. Lutz, et al., A versatile valving toolkit for automating fluidic operations in paper microfluidic devices, Lab Chip 15 (2015) 1432–1444. Available from http://xlink.rsc.org/?DOI=C4LC01155D.
[84] H. Chen, J. Cogswell, C. Anagnostopoulos, M. Faghri, A fluidic diode, valves, and a sequential-loading circuit fabricated on layered paper, Lab Chip 12 (2012) 2909. Available from http://xlink.rsc.org/?DOI=c2lc20970e.
[85] R. Gerbers, W. Foellscher, H. Chen, C. Anagnostopoulos, M. Faghri, A new paper-based platform technology for point-of-care diagnostics, Lab Chip 14 (2014) 4042–4049. Available from http://xlink.rsc.org/?DOI=C4LC00786G.
[86] X. Wei, T. Tian, S. Jia, Z. Zhu, Y. Ma, J. Sun, et al., Target-responsive DNA hydrogel mediated stop-flow microfluidic paper-based analytic device for rapid, portable and visual detection of multiple targets, Anal. Chem. 87 (2015) 4275–4282.
[87] Statista, Number of Smartphone Subscriptions Worldwide From 2016 to 2027, 2022, [cited 2002 Jun 22]; Available from https://www.statista.com/statistics/330695/number-of-smartphone-users-worldwide/.
[88] S. Smith, J.G. Korvink, D. Mager, K. Land, The potential of paper-based diagnostics to meet the ASSURED criteria, RSC Adv. 8 (2018) 34012–34034.
[89] A.W. Martinez, S.T. Phillips, E. Carrilho, S.W. Thomas, H. Sindi, G.M. Whitesides, Simple telemedicine for developing regions: camera phones and paper-based microfluidic devices for real-time, off-site diagnosis, Anal. Chem. 80 (2008) 3699–3707.
[90] L. Shen, M. Ratterman, D. Klotzkin, I. Papautsky, Use of a low-cost CMOS detector and cross-polarization signal isolation for oxygen sensing, IEEE Sensors J. 11 (2011) 1359–1360.
[91] B. Nelis, B. Zhao, E. Rafferty, et al., The efficiency of color space channels to quantify color and color intensity change in liquids, pH strips, and lateral flow assays with smartphones, Sensors 19 (2019) 5104. Available from https://www.mdpi.com/1424-8220/19/23/5104.
[92] J. Guo, J.X.H. Wong, C. Cui, X. Li, H.Z. Yu, A smartphone-readable barcode assay for the detection and quantitation of pesticide residues, Analyst 140 (2015) 5518–5525.
[93] K. Cantrell, M.M. Erenas, I. De Orbe-Payá, L.F. Capitán-Vallvey, Use of the hue parameter of the hue, saturation, value color space as a quantitative analytical parameter for bitonal optical sensors, Anal. Chem. 82 (2010) 531–542.
[94] R. Yang, W. Cheng, X. Chen, Q. Qian, Q. Zhang, Y. Pan, et al., Color space transformation-based smartphone algorithm for colorimetric urinalysis, ACS Omega 3 (2018) 12141–12146.
[95] CIE. CIE 015:2018, Colorimetry, fourth ed., 2018. Vienna. Available from: https://cie.co.at/publications/colorimetry-4th-edition.
[96] H. Karlsen, T. Dong, Illumination and device independence for colorimetric detection of urinary biomarkers with smartphone, in: In: 2016 38th Annual International Conference of the IEEE Engineering in Medicine and Biology Society (EMBC), IEEE, 2016, pp. 5184–5187. Available from http://ieeexplore.ieee.org/document/7591895/.
[97] A. Gräwe, A. Dreyer, T. Vornholt, U. Barteczko, L. Buchholz, G. Drews, et al., A paper-based, cell-free biosensor system for the detection of heavy metals and date rape drugs, PLoS One 14 (2019) e0210940.

[98] J.D. Pédelacq, S. Cabantous, T. Tran, T.C. Terwilliger, G.S. Waldo, Engineering and characterization of a superfolder green fluorescent protein, Nat. Biotechnol. 24 (2006) 79–88. Available from https://www.nature.com/articles/nbt1172.
[99] L.H. Chen, R. Steffen, SARS-CoV-2 testing to assure safety in air travel, J. Travel Med. 28 (2021) 1–4. Available from https://academic.oup.com/jtm/article/doi/10.1093/jtm/taaa241/6067290.
[100] V. Dhanasekaran, K.M. Edwards, R. Xie, H. Gu, D.C. Adam, L.D.J. Chang, et al., Air travel-related outbreak of multiple SARS-CoV-2 variants, J. Travel Med. 28 (2021) 1–7. Available from https://academic.oup.com/jtm/article/doi/10.1093/jtm/taab149/6372544.
[101] J. Matthews, R. Kulkarni, M. Gerla, T. Massey, Rapid dengue and outbreak detection with mobile systems and social networks, Mobile Netw. Appl. 17 (2012) 178–191.
[102] W. Dungchai, O. Chailapakul, C.S. Henry, Electrochemical detection for paper-based microfluidics, Anal. Chem. 81 (2009) 5821–5826. Available from https://pubs.acs.org/doi/10.1021/ac9007573.
[103] A.C. Sun, C. Yao, A.G. Venkatesh, D.A. Hall, An efficient power harvesting mobile phone-based electrochemical biosensor for point-of-care health monitoring, Sensors Actuators B Chem. 235 (2016) 126–135. Available from: https://linkinghub.elsevier.com/retrieve/pii/S092540051630675X.
[104] E. Aronoff-Spencer, A.G. Venkatesh, A. Sun, H. Brickner, D. Looney, D.A. Hall, Detection of Hepatitis C core antibody by dual-affinity yeast chimera and smartphone-based electrochemical sensing, Biosens. Bioelectron. 86 (2016) 690–696. Available from: https://doi.org/10.1016/j.bios.2016.07.023.
[105] J. Aymerich, A. Márquez, L. Terés, X. Muñoz-Berbel, C. Jiménez, C. Domínguez, et al., Cost-effective smartphone-based reconfigurable electrochemical instrument for alcohol determination in whole blood samples, Biosens. Bioelectron. 117 (2018) 736–742.
[106] D. Zhang, Y. Lu, Q. Zhang, L. Liu, S. Li, Y. Yao, et al., Protein detecting with smartphone-controlled electrochemical impedance spectroscopy for point-of-care applications, Sensors Actuators B Chem. 222 (2016) 994–1002.
[107] Microsoft, Windows 10 Mobile End of Support FAQ, 2022, [cited 2022 Jun 22]; Available from https://support.microsoft.com/en-gb/windows/windows-10-mobile-end-of-support-faq-8c2dd1cf-a571-00f0-0881-bb83926d05c5.
[108] BlackBerry, BlackBerry 10 and BlackBerry OS Services FAQ, 2022, [cited 2022 Jun 22]; Available from https://www.blackberry.com/us/en/support/devices/end-of-life.
[109] E.M. Benjamin, Self-monitoring of blood glucose: the basics, Clin. Diabetes 20 (2002) 45–47. Available from https://diabetesjournals.org/clinical/article/20/1/45/746/Self-Monitoring-of-Blood-Glucose-The-Basics.
[110] S. Denford, A.F. Martin, N. Love, D. Ready, I. Oliver, R. Amlôt, et al., Engagement with daily testing instead of self-isolating in contacts of confirmed cases of SARS-CoV-2: a qualitative analysis, Front. Public Health 9 (2021) 1–11.
[111] S.K. Gupta, Medical device regulations: a current perspective, J. Young Pharm. 8 (2015) 06–11. Available from http://jyoungpharm.org/article/822.
[112] S. Lamph, Regulation of medical devices outside the European Union, J. R. Soc. Med. 105 (2012) 12–21. Available from http://journals.sagepub.com/doi/10.1258/jrsm.2012.120037.
[113] A.V. Kaplan, D.S. Baim, J.J. Smith, D.A. Feigal, M. Simons, D. Jefferys, et al., Medical device development, Circulation 109 (2004) 3068–3072. Available from https://www.ahajournals.org/doi/10.1161/01.CIR.0000134695.65733.64.
[114] The European Parliament and the Council of the European Union, Regulation (EU) 2017/746 of the European Parliament and of the Council of 5 April 2017 on in Vitro Diagnostic Medical Devices and Repealing Directive 98/79/EC and Commission Decision 2010/227/EU. Off. J. Eur. Union, 2017.

[115] B.R. Lubbers, A. Schilhabel, C.M. Cobbaert, D. Gonzalez, I. Dombrink, M. Brüggemann, et al., The New EU regulation on in vitro diagnostic medical devices: implications and preparatory actions for diagnostic laboratories, HemaSphere 5 (2021) e568. Available from https://journals.lww.com/10.1097/HS9.0000000000000568.

[116] European Commission, Regulation (EC) No 853/2004 of the European Parlamient and of the Council of 29 April 2004 Laying Down Specific Hygiene Rules for on the Hygiene of Foodstuffs, Off. J. Eur. Union L 139 (2004) 55.

[117] The European Parliament and the Council of the European Union, Commission Regulation (EU) No 519/2014 of 16 May 2014 Amending Regulation (EC) No 401/2006 as Regards Methods of Sampling of Large Lots, Spices and Food Supplements, Performance Criteria for T-2, HT-2 Toxin and Citrinin and Screening Methods of Analysis. Off. J. Eur. Union, 2014.

[118] Food Standards Act 1999. 1999.

[119] M. Dillon, M.A. Zaczek-Moczydlowska, C. Edwards, A.D. Turner, P.I. Miller, H. Moore, et al., Current trends and challenges for rapid SMART diagnostics at point-of-site testing for marine toxins, Sensors 21 (2021) 2499. Available from https://www.mdpi.com/1424-8220/21/7/2499.

[120] J.J. Dorantes-Aranda, J.Y.C. Tan, G.M. Hallegraeff, K. Campbell, S.C. Ugalde, D.T. Harwood, et al., Detection of paralytic shellfish toxins in mussels and oysters using the qualitative neogen lateral-flow immunoassay: an interlaboratory study, J. AOAC Int. 101 (2018) 468–479. Available from https://academic.oup.com/jaoac/article/101/2/468-479/5653938.

[121] A.K. Yetisen, J.L. Martinez-Hurtado, V.F. da Cruz, M.C.E. Simsekler, M.S. Akram, C.R. Lowe, The regulation of mobile medical applications, Lab Chip 14 (2014) 833. Available from http://xlink.rsc.org/?DOI=c3lc51235e.

[122] C.J. Vincent, G. Niezen, A.A. O'Kane, K. Stawarz, Can standards and regulations keep up with health technology? JMIR Mhealth Uhealth 3 (2015), e64. Available from http://mhealth.jmir.org/2015/2/e64/.